Estuarine, Coastal and Shelf Science 181 (2016) 123–133

Contents lists available at ScienceDirect

Estuarine, Coastal and Shelf Science

journal homepage: www.elsevier.com/locate/ecss

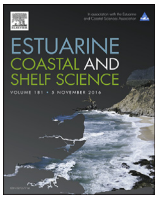

Variability of the Antarctic Coastal Current in the Amundsen Sea

Chang-Sin Kim [a], Tae-Wan Kim [a, *], Kyoung-Ho Cho [a], Ho Kyung Ha [b], SangHoon Lee [a], Hyun-Cheol Kim [a], Jae-Hak Lee [c]

[a] Korea Polar Research Institute, Incheon, South Korea
[b] Department of Ocean Sciences, Inha University, Incheon, South Korea
[c] Korea Institute of Ocean Science and Technology, Ansan, South Korea

ARTICLE INFO

Article history:
Received 27 December 2015
Received in revised form
8 August 2016
Accepted 10 August 2016
Available online 11 August 2016

Keywords:
Antarctic Coastal Current (AACC)
Variability
Ekman vertical velocity
Dotson Ice Shelf
Amundsen Sea

ABSTRACT

The nature of the Antarctic Coastal Current (AACC) and its seasonal and non-seasonal (several-day) variability were investigated using long-term mooring data obtained near the Dotson Ice Shelf in the Amundsen Sea. The moored instruments were operated from February 2012 to January 2014 in the Dotson Trough, which is one of the deep troughs on the Amundsen Sea shelf. The hydrographic structure of sigma density distribution at the ice shelf (27.25 kg m^{-3} at the surface) was found to be higher than at the continental shelf (27.00 kg m^{-3}), whereas in the middle layer, 27.45 kg m^{-3} isopycnal extended to 300 m depth near the ice shelf but below 200 m depth in the offshore. The surface mixed layer thickened from the shelf break toward the ice shelf. This thickening was caused partially by coastal downwelling resulting from onshore Ekman transport and by Ekman pumping in the coastal area. The baroclinic component of the AACC near the Dotson Ice Shelf increased from July to October and decreased from January to June in 2013. In comparison with other potential driving forces, the seasonal and non-seasonal (short-term) variation of the AACC correlated well with density variability, determined principally by salinity variation. Therefore, it is suggested that the variability of the isopycnocline by Ekman pumping in the coastal area is one of the important factors controlling the seasonality and non-seasonal variability of the AACC.

1. Introduction

The ice sheet around West Antarctica has experienced widespread loss over recent decades (Bindschadler, 2006; Rignot et al., 2008; Dutrieux et al., 2014); a change that could contribute to global sea level rise (Scambos et al., 2004; Pritchard and Vaughan, 2007; Joughin et al., 2010). The Amundsen Sea is one region of West Antarctica that has changed most rapidly. Several studies have suggested that oceanic heat transport to the ice shelves by intrusion of warm Circumpolar Deep Water can contribute to the increase in basal melt rate (Walker et al., 2007; Jenkins et al., 2010; Wåhlin et al., 2010; Jacobs et al., 2011, 2012; Arneborg et al., 2012; Nakayama et al., 2013; Dutrieux et al., 2014; Ha et al., 2014).

The Antarctic Coastal Current (AACC; ACoC) is one of the interesting features of the Southern Ocean. Globally, it is the southernmost current, representing the subpolar regime, the entire region south of the Antarctic Circumpolar Current and flows in a westward direction parallel with the Antarctic continent (Orsi et al., 1995; Whitworth et al., 1998; Mathiot et al., 2011). Sverdrup (1953) reported the first direct observations of the current along the Antarctic continental slope, which revealed a westward flow in the Weddell Sea. Whitworth et al. (1998) suggested the characteristics of the AACC change from a broad flow far from the coast to a narrow flow close to the coast. In the narrow continental shelf area, it is difficult to distinguish the locations of the AACC and Antarctic Slope Front (Heywood et al., 1998, 2004). The AACC is a fast and shallow flow in the continental shelf area and it is often associated with the front of the ice shelf (Jacobs, 1991; Heywood et al., 2004).

The strong westward flows of the AACC and Antarctic Shelf Front affect the dynamics of the ocean environment, such as the water masses and circulations in the area of the Antarctic continental shelf (Whitworth et al., 1998; Mathiot et al., 2011). Strong coastal currents flowing along the edge of the ice shelf increase the exchange of heat and mass at the seawater–ice shelf interface, accelerating the rate of ice shelf melt (Hellmer et al., 2012). Nakayama et al. (2014) established that the consequent dispersion

---

* Corresponding author.
E-mail address: twkim@kopri.re.kr (T.-W. Kim).

http://dx.doi.org/10.1016/j.ecss.2016.08.004
0272-7714/© 2016 Elsevier Ltd. All rights reserved.

of ice shelf meltwater affects the ocean surface circulation and the formation of water masses. Their numerical simulations suggested that a slight increase in the rate of basal mass loss of the ice shelves of the Amundsen and Bellingshausen seas could substantially increase the transport of meltwater into the Ross Sea, by strengthening the melt-driven shelf circulation and westward coastal current.

The westward AACC is driven by wind stress and buoyancy forcing (Tchernia and Jeannin, 1980; Tchernia, 1981; Núñez-Riboni and Fahrbach, 2009; Combes and Matano, 2014). Núñez-Riboni and Fahrbach (2009) revealed four driving mechanisms that may potentially determine the seasonal variability of the AACC's barotropic and baroclinic components in the Weddell Sea. Wind-driven Ekman transport accounts for 58% of the total barotropic variation of the coastal current (Núñez-Riboni and Fahrbach, 2009), and the density gradient due to the presence of fresh and cool meltwater near the ice shelf between the Antarctic Surface Water (AASW) and Shelf Water represents its baroclinic component (Fahrbach et al., 1992). Ekman transport is related to wind stress, however, sea ice concentration affects the momentum transfer between the wind and the current by modifying the surface drag coefficient (Fennel and Johannessen, 1998; Lüpkes and Birnbaum, 2005).

The variability of the AACC in the Amundsen Sea is understood only superficially because of the relative dearth of measurements in this region. Moreover, the AACC in the Amundsen Sea advances in the non-slope region and it appears nearby the ice shelf. Quantifying the effect of each forcing on the variability of the AACC and on its barotropic and baroclinic components is necessary for fuller understanding of the dynamics of the AACC (Núñez-Riboni and Fahrbach, 2009). We undertook a summertime cruise in 2012 and 2014 onboard the icebreaker R/V *Araon* and obtained hydrographic data on a transect along the Dotson Trough, which included the Amundsen Sea polynya and sea ice region (Fig. 1). We also collated two years' data recorded by instruments moored near the Dotson Ice Shelf. Using these observational datasets, the objective of this study was to quantify the contributions of the driving mechanisms to the seasonality and non-seasonal (short-term) fluctuation of the coastal current in the Amundsen Sea. Specifically, we investigated the forces that contribute to the seasonal and non-seasonal variability of the AACC, and we considered how the hydrographic state affects the intensity of the AACC and what causes the hydrographic state to change.

This remainder of this paper is organized as follows. Section 2 describes information relevant to the observations and method used in the investigation. Section 3.1 describes the hydrographic condition of the westward AACC in austral summer and its long-term variation. Section 3.2 describes the seasonal variation of the AACC and its possible forcings. Section 3.3 describes the relationship between the AACC and non-seasonal variation of wind and density. Section 4.1 introduces a more specific description of the dynamics of the ocean circulation in the coastal area of Antarctica. Section 4.2 describes the weakening of the westward AACC by the baroclinic effect. Section 4.3 describes the relationship between the coastal current and Ekman pumping velocity. Our findings are summarized in Section 5.

2. Materials and methods

2.1. Data

Oceanic data were collected during hydrographic surveys and from moored stations (Fig. 1). Conductivity–temperature–depth (CTD) sensors (SeaBird Electronics 911+) were used to measure the background hydrographic structures (i.e., potential temperature and salinity), and the vertical profiles of current data were observed using a 300-kHz lowered acoustic Doppler current profiler (LADCP; Teledyne RD Instruments).

The long-term data were collated by the moored stations from February 2012 to January 2014. To measure the temporal variability of potential temperature, salinity, and velocity, two moored stations were deployed in the study area (red circles in Fig. 1): K1 at the entrance of the continental shelf and K3 nearby the ice shelf. The water depths of K1 and K3 are about 525 m and 1057 m, respectively. The instruments deployed at these moored stations comprised of five recording current meters (RCM 11, accuracy: ±0.15 cm/s) and four MicroCAT (SBE37 SM) instruments to measure temperature (accuracy: ±0.002 K) and conductivity (accuracy: ±0.0003 S/m). The RCMs were deployed at depths of 250 and 400 m at K1 and 220, 490, and 850 m at K3. The potential temperature and salinity observations were taken at depths of 250 and 400 m at K1 and 220 and 845 m at the K3 station. The LADCP data and long-term RCM data were processed using the same technique as Thurnherr (2010), and the water velocities were detided with the major 10 harmonic components using the barotropic tide model (Padman et al., 2002).

To identify the effects of atmospheric forcing and sea ice on the coastal current, wind and sea ice concentration (SIC) data were obtained from the European Centre for Medium-Range Weather Forecasts (ECMWF) ERA-Interim and the Special Sensor Microwave Imager/Sounder (SSMIS) of the Defense Meteorological Satellite Program (DMSP), respectively. Daily averages of the 6-hourly reanalysis wind data were determined for comparison with other daily variables (i.e., SIC). The horizontal grid resolution of the wind and SIC data were 0.25° and 3 km, respectively. We considered the isoline of 15% SIC as the division between the seasonal ice zone (SIZ) and a polynya. Fig. 1 shows the SIZ (interior area of the white hachured line) and the Amundsen Sea Polynya (un-hachured region; ice area in the south of the Amundsen Sea) averaged between January 12–16, 2012 (period of hydrographic observation). The direction of small white tick marks or hachures on the contour lines indicates greater SIC. To identify the effects of ocean stress, sea ice velocity data were taken from the Polar Pathfinder Daily 25 km EASE-Grid Sea Ice Motion Vectors Version 3 (Tschudi et al., 2016), which has horizontal resolution of 25 km.

In order to understand the dynamics of the AACC, we divided the baroclinic component from the current velocity, despite only having observations from three layers, using a similar method to Núñez-Riboni and Fahrbach (2009). The barotropic component was calculated as the vertical mean velocity of a spline-fitted vertical profile using the time series data from the three layers recorded by the moored stations. The baroclinic component for each level was considered by subtracting the barotropic component from each time series. Although this method for separating the barotropic component from the coastal current has some uncertainty, the calculated baroclinic component was sufficient to establish the cause of the seasonal variation of the AACC.

We conducted two analyses of the time series data to determine the seasonal and non-seasonal variations. To understand the seasonal cycle of the AACC, we subtracted the seasonal cycle of the local wind, SIC, wind stress curl, and moored hydrographic data using Butterworth low-pass filter lines with a cut-off period of 90 days, similar to Núñez-Riboni and Fahrbach (2009). To compare the short-term fluctuations, we calculated the time series of wind stress, density, and current velocity anomalies, which were subsequently reprocessed using the Butterworth band-pass filter with cut-off periods of between 7 and 90 days, to remove micro- and macro-scale (tides and seasonality) variations.